Cell Research (2013) 23:658-672.

www.nature.com/cr

ORIGINAL ARTICLE

Rapid and efficient reprogramming of human fetal and adult blood CD34$^+$ cells into mesenchymal stem cells with a single factor

Xianmei Meng[1, *], Rui-Jun Su[2, 3, *], David J Baylink[1], Amanda Neises[1], Jason B Kiroyan[1], Wayne Yuk-Wai Lee[4], Kimberly J Payne[2, 3], Daila S Gridley[5], Jun Wang[6], K-H William Lau[7], Gang Li[4], Xiao-Bing Zhang[1]

[1]Division of Regenerative Medicine MC1528B, Department of Medicine, Loma Linda University, Loma Linda, CA 92354, USA; [2]Division of Anatomy, Loma Linda University, Loma Linda, CA 92354, USA; [3]Center for Health Disparities and Molecular Medicine, Loma Linda University, Loma Linda, CA 92354, USA; [4]Stem Cells and Regeneration Program, School of Biomedical Sciences, Department of Orthopaedics and Traumatology, Li Ka Shing Institute of Health Sciences, The Chinese University of Hong Kong, Prince of Wales Hospital, Shatin, Hong Kong SAR, China; [5]Department of Radiation Medicine, Loma Linda University, Loma Linda, CA 92354, USA; [6]Department of Pathology, Loma Linda University, Loma Linda, CA 92354, USA; [7]Musculoskeletal Disease Center, Jerry L Pettis Memorial VA Medical Center, Loma Linda, CA 92354, USA

The direct conversion of skin cells into somatic stem cells has opened new therapeutic possibilities in regenerative medicine. Here, we show that human induced mesenchymal stem cells (iMSCs) can be efficiently generated from cord blood (CB)- or adult peripheral blood (PB)-CD34$^+$ cells by direct reprogramming with a single factor, OCT4. In the presence of a GSK3 inhibitor, 16% of the OCT4-transduced CD34$^+$ cells are converted into iMSCs within 2 weeks. Efficient direct reprogramming is achieved with both episomal vector-mediated transient OCT4 expression and lentiviral vector-mediated OCT4 transduction. The iMSCs express MSC markers, resemble bone marrow (BM)-MSCs in morphology, and possess *in vitro* multilineage differentiation capacity, yet have a greater proliferative capacity compared with BM-MSCs. Similar to BM-MSCs, the implanted iMSCs form bone and connective tissues, and are non-tumorigenic in mice. However, BM-MSCs do not, whereas iMSCs do form muscle fibers, indicating a potential functional advantage of iMSCs. In addition, we observed that a high level of OCT4 expression is required for the initial reprogramming and the optimal iMSC self-renewal, while a reduction of OCT4 expression is required for multilineage differentiation. Our method will contribute to the generation of patient-specific iMSCs, which could have applications in regenerative medicine. This discovery may also facilitate the development of strategies for direct conversion of blood cells into other types of cells of clinical importance.

Keywords**:** mesenchymal stem cells; hematopoietic cells; direct reprogramming; CD34$^+$ cells
Cell Research (2013) **23**:658-672. doi:10.1038/cr.2013.40; published online 12 March 2013

Introduction

Mesenchymal stem cells (MSCs) are somatic stem cells responsible for the regeneration of cartilage, tendon, ligament, muscle and bone, and thus hold great promise for treating skeletal diseases [1-5]. Due to their immunomodulatory potential, MSCs have also been used in clinical and preclinical studies to treat multiple diseases including graft versus host disease (GVHD) [6], Crohn's disease [7], organ transplant rejection [8] and diabetes [9]. MSCs can be isolated from multiple tissues like bone marrow (BM) and adipose tissue [10]. However, the procedures are invasive and often yield limited numbers of MSCs for therapy. MSCs differentiated from human induced pluripotent stem cells (iPSCs) have been used for skeletal regeneration and tissue repair [11-13]. However, this approach is time-consuming, and the risk

*These two authors contributed equally to this work.
Correspondence: Xiao-Bing Zhang
Tel: +1-909-651-5886; Fax: +1-909-558-0428
E-mail: xzhang@llu.edu
Received 15 November 2012; revised 19 December 2012; accepted 13 January 2013; published online 12 March 2013

of teratoma formation due to trace amount of undifferentiated or contaminated iPSCs in iPSC-MSCs remains a concern. Thus, the direct reprogramming of somatic cells into MSCs presents an alternative to the iPSC approach and might decrease the risk of teratoma formation.

The direct reprogramming of one type of cells, most commonly fibroblasts, into another by ectopic expression of defined transcription factors has recently been achieved. Successful reprogramming of human or mouse fibroblasts into neural stem cells [14-15], cardiomyocytes [16-17] and hepatocytes [18-19] has been reported. The most readily available cell sources of adult human are skin and blood. The use of blood cells for reprogramming has unique advantages over dermal fibroblasts, as blood cells likely harbor fewer acquired genetic mutations induced by environmental insults, and can be easily obtained from patients with minimal invasiveness [20-23]. The first report of direct reprogramming of blood cells into somatic cells of clinical interest, such as neuronal cells, has recently been published [24]. Cord blood (CB)-$CD133^+$ progenitor cells are reprogrammed to neuronal cells by ectopic expression of SOX2 and MYC at an efficiency of < 0.1%, requiring 3 weeks for the generation of neuronal cell-like colonies [24]. In addition, the use of the oncogene MYC poses a serious risk of tumorigenesis. Thus, we have been interested in identifying an approach that can generate MSCs safely, rapidly and efficiently from blood cells. Here, we present a novel approach for generating self-renewable, multipotent and non-tumorigenic induced mesenchymal stem cells (iMSCs) from human blood $CD34^+$ cells by direct reprogramming with only one factor.

Results

Generation of iMSCs from CB-$CD34^+$ cells

We have previously reported the efficient generation of iPSCs from human CB-$CD34^+$ cells with a single vector that expresses OCT4 and SOX2 (Lenti SFFV-OCT4-2A-SOX2) [25]. When the two factors were expressed by two individual lentiviral vectors (Lenti SFFV-OCT4 and Lenti SFFV-SOX2), we observed that ~80% of the colonies morphologically resemble mesenchymal cells. This finding prompted us to explore whether OCT4 or SOX2 alone can reprogram $CD34^+$ cells directly into MSC-like cells, which we term as induced MSCs (iMSCs) hereafter for brevity. We found that transduction of CB-$CD34^+$ cells with Lenti SFFV-OCT4, but not Lenti SFFV-SOX2, induced iMSC formation (Supplementary information, Figure S1A), suggesting that OCT4 is responsible for the induced cell fate conversion. We also tested other reprogramming factors and found that MYC, NANOG, KLF4, LIN28 or TBX3 alone completely failed to convert CB-$CD34^+$ cells into iMSCs (Supplementary information, Figure S1B). Furthermore, the combination of these factors with OCT4 did not significantly increase the reprogramming efficiency. Thus, our subsequent studies focused on OCT4 only.

A successful iMSC conversion depends on OCT4 overexpression and MSC-conducive culture conditions. The transduction of CB-$CD34^+$ cells with green fluorescent protein (GFP) control did not generate MSCs (Figure 1A and Supplementary information, Video S1), whereas OCT4-transduced cells formed colonies and were transformed morphologically into spindle-like cells within 3-4 days of culture in MSC-conducive conditions (Figure 1B and Supplementary information, Video S2). Some OCT4-transduced cells cultured in hematopoietic stem cell (HSC) medium manifested a spindle-like morphology, but died shortly after the formation of small colonies (Figure 1C and Supplementary information, Video S3). We also found that the use of human fibronectin-precoated non-tissue culture-treated (non-TC) culture plates that allow for efficient attachment of transduced CB-$CD34^+$ cells is crucial for the rapid morphological transformation (1 week), whereas in the absence of fibronectin, the morphological transformation takes 2-3 weeks.

To optimize the reprogramming protocol, we tested whether small molecules capable of enhancing the reprogramming of somatic cells into iPSCs, such as GSK3 inhibitor CHIR99021 (CHIR), MEK inhibitor and ALK5 inhibitor, can also increase the efficiency of direct reprogramming of CB-$CD34^+$ cells into iMSCs. After a series of experiments, we found that only CHIR can substantially enhance the reprogramming process; it increased the reprogramming efficiency from 3% to 16% (Figure 1D and 1E). Colonies were also substantially larger in size in the presence of CHIR (Figure 1D). Moreover, CHIR consistently increased the iMSC proliferation rate in long-term cultures (Figure 1F), and shortened the population doubling time from 35 h to 20 h. These data demonstrate that CHIR increases both the reprogramming efficiency and the *in vitro* proliferative rate of iMSCs.

The transition of CB-$CD34^+$ cells to phenotypically mature iMSCs takes several weeks. During the first 2 weeks of the transdifferentiation, cells expressing the pan-hematopoietic marker, CD45, steadily decreased from > 99% to < 1%, whereas cells expressing the MSC marker, CD73, rapidly increased from 0% to > 70% (Figure 1G and Supplementary information, Figure S2A). MSC markers CD29 and CD44 were also expressed in HSCs, but at low levels. Of interest, we observed a 15-fold and 6-fold increase of the expression of CD29 and CD44, respectively, over 3-4 weeks (Supplementary

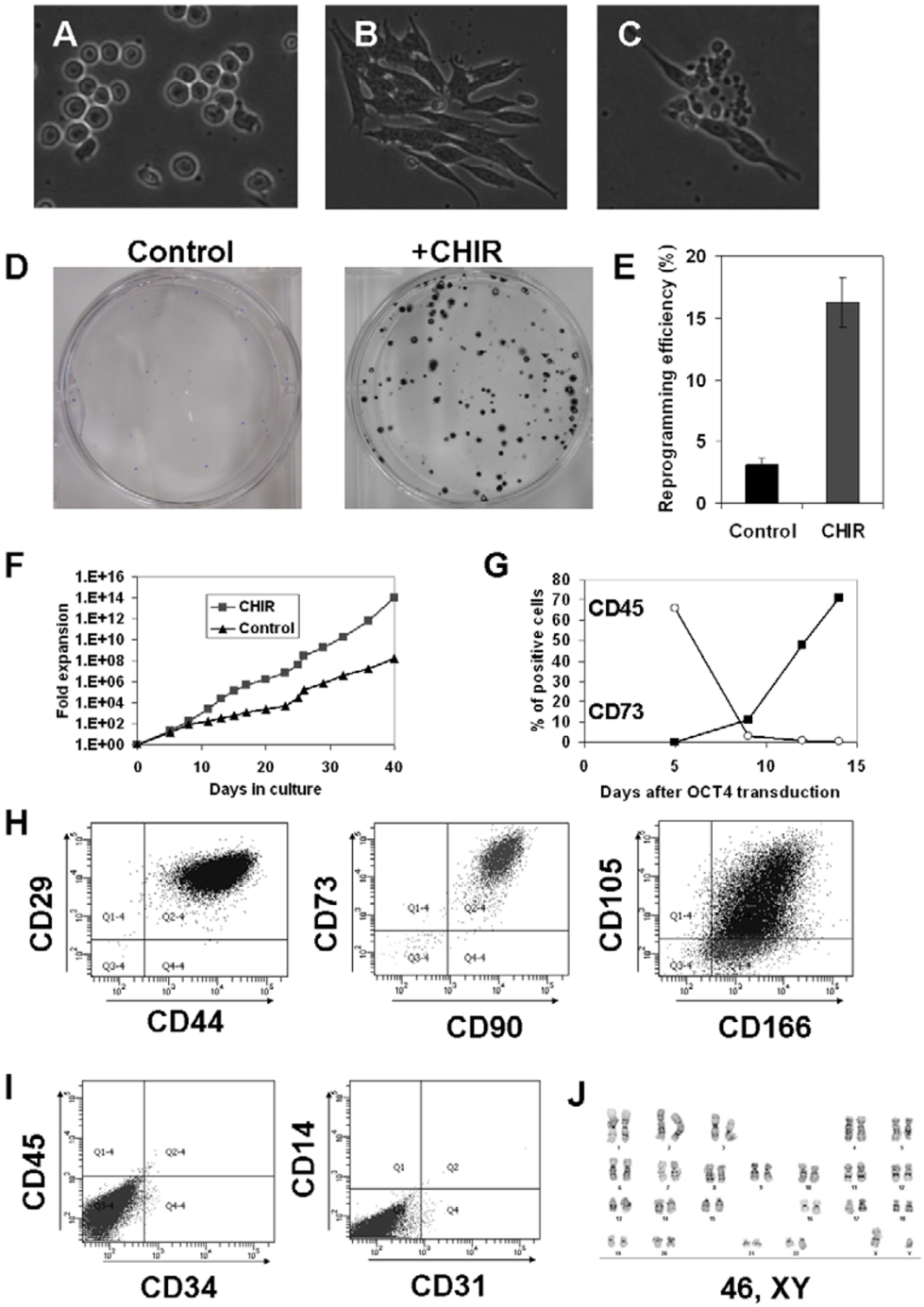

Figure 1 OCT4-transduced human CB-CD34$^+$ cells give rise to MSC-like cells. **(A-C)** CB-CD34$^+$ cells transduced with the GFP control vector retained the hematopoietic morphology at 5 days post-transduction **(A)**. OCT4-transduced CB-CD34$^+$ cells developed a MSC-like morphology when cultured in MSC medium **(B)**, but the MSC-like cells did not survive when cultured in HSC medium **(C)**. **(D)** Colony formation at 9 days after seeding 1 000 OCT4-transduced CB-CD34$^+$ cells in MSC culture conditions with or without CHIR. **(E)** Reprogramming efficiency with and without CHIR (n = 3, P < 0.01). Error bars indicate SEM. **(F)** iMSC fold expansion over time shows that CHIR promotes long-term *in vitro* proliferation of reprogrammed iMSCs. Data shown are a representative of 3 independent experiments with similar results. **(G)** Changes in the percentage of cells expressing the pan-hematopoietic marker CD45 and the MSC marker CD73, as measured by flow cytometry of OCT4-transduced cells over time. **(H)** Flow cytometry plots of typical MSC marker expression assessed at 1 month after OCT4 transduction. **(I)** Flow cytometry plots for expression of blood cell markers (CD45, CD14 and CD34) and endothelial cell marker CD31 assessed at 1 month after OCT4 transduction. **(J)** iMSCs show a normal karyotype after 3 months of culture.

information, Figure S2B-S2D). Four weeks after Lenti SFFV-OCT4 transduction, almost all the cells expressed typical MSC markers: CD29, CD44, CD73, CD90, CD105 and CD166 (Figure 1H), whereas the expression of the hematopoietic markers CD45, CD34 and CD14, or the endothelial marker CD31 was negligible (Figure 1I). These data provide evidence that fully reprogrammed iMSCs are phenotypically identical to MSCs from other sources.

OCT4-reprogrammed iMSCs are genetically stable and do not form tumors

We further examined the *in vitro* long-term proliferative capacity and potential risk of tumor formation of iMSCs. In five independent experiments, the iMSCs expanded robustly over the 4 months of culture, with a cell population doubling time of 20-22 h in the presence of CHIR (Supplementary information, Figure S3). Of note, the rate of cellular proliferation was virtually unchanged during the entire period of culture, with no signs of senescence or transformation based on the frequency of cell division. We asked whether OCT4 expression induces genomic instability after long-term *in vitro* culture. Karyotype analysis did not detect any major chromosomal abnormalities (Figure 1J). To further investigate the safety of these cells, we injected 1-2 $\times$ 10^6 iMSCs systemically or subcutaneously into 20 immunodeficient mice. Unlike iPSCs [25], iMSCs did not form tumors during 3 months of follow-up. In comparison, injection of iMSCs that were generated with OCT4 and MYC led to tumor formation at 1 month after systemic or subcutaneous inoculation (data not shown). These data suggest that the use of OCT4 for direct reprogramming of CB-CD34$^+$ cells into iMSCs is a safe approach for rapid generation of large quantities of MSCs.

iMSCs are reprogrammed directly from hematopoietic progenitors, not from mature myeloid cells

As MSCs are present in the CB at frequencies ranging from 0 to 2.3 clones per 1 $\times$ 10^8 mononuclear cells or ~0.1 clones per ml [26], we asked whether OCT4 expands the contaminated MSCs in CB-CD34$^+$ cells rather than directly reprogramming hematopoietic cells into iMSCs. The proliferation of the existing MSCs in the CB cannot explain iMSC generation, as no MSCs were generated from nontransduced CB-CD34$^+$ cells after 2-3 weeks of culture under our MSC culture conditions. To unambiguously test this possibility, we cloned single CB-CD34$^+$ cells in U-bottomed 96-well plates. After 10 days of culture in medium supplemented with cytokines TPO, SCF, FL, IL-3 and G-CSF, hematopoietic cell colonies were formed in ~10% of the wells (Supplementary information, Figure S4). Random selection of 12 clones, followed by transduction with Lenti SFFV-OCT4 led to the formation of iMSCs in 33% cases (Supplementary information, Figure S4). These data demonstrate that iMSCs are directly reprogrammed from hematopoietic cells. Of interest, when CB-CD34$^+$ cells were cultured in the condition that promotes myeloid differentiation for 20 days before OCT4-transduction, no iMSC colonies were generated from 12 randomly selected individual clones (data not shown). These data suggest that OCT4 likely reprograms hematopoietic progenitors into iMSCs, but cells in the terminal stages of myeloid differentiation cannot be reprogrammed by OCT4 overexpression.

Reprogramming to iMSCs requires a high level of OCT4 expression and lacks an iPSC stage

Next, we examined the potential mechanisms of OCT4-mediated direct reprogramming from CB-CD34$^+$ cells into iMSCs. Consistent with our previous report [25], we found that the iMSC reprogramming critically depends on OCT4 expression levels. When we used a relatively weak promoter such as EF1α or PGK that leads to 50%-60% lower expression of OCT4 compared to the SFFV promoter in hematopoietic cells [25], the reprogramming from CB-CD34$^+$ cells into iMSCs completely failed. This result suggests that a high level of OCT4 expression is necessary for the successful reprogramming of hematopoietic cells.

We then asked whether a pluripotent state is induced during the transdifferentiation process. Apart from OCT4, whose expression level is similar to that in iPSCs (Figure 2A and Supplementary information, Figure S5), other pluripotency markers, such as SOX2, NANOG and TRA-1-60 were undetectable in iMSCs (Figure 2A). Bisulphite sequencing showed that *OCT4* and *NANOG* promoters are hypermethylated (Figure 2B), suggesting that the endogenous *OCT4* gene is not activated in iMSCs. We also found that OCT4 alone is insufficient for the reprogramming of CB-CD34$^+$ cells into iPSCs and that the culture of iMSCs in iPSC-conducive conditions does not lead to the formation of iPSC colonies (Figure 2C and 2D). Taken together, our data suggest that reprogramming of CB-CD34$^+$ cells into iMSCs does not go through an iPSC stage.

A high level of OCT4 expression inhibits iMSC differentiation

MSCs have the capacity to differentiate into adipocytes, osteoblasts and chondrocytes in differentiation-inducing conditions. However, iMSCs generated by transduction with the lentiviral vector SFFV-OCT4 (Lenti iMSCs) failed to differentiate into mature progenies of

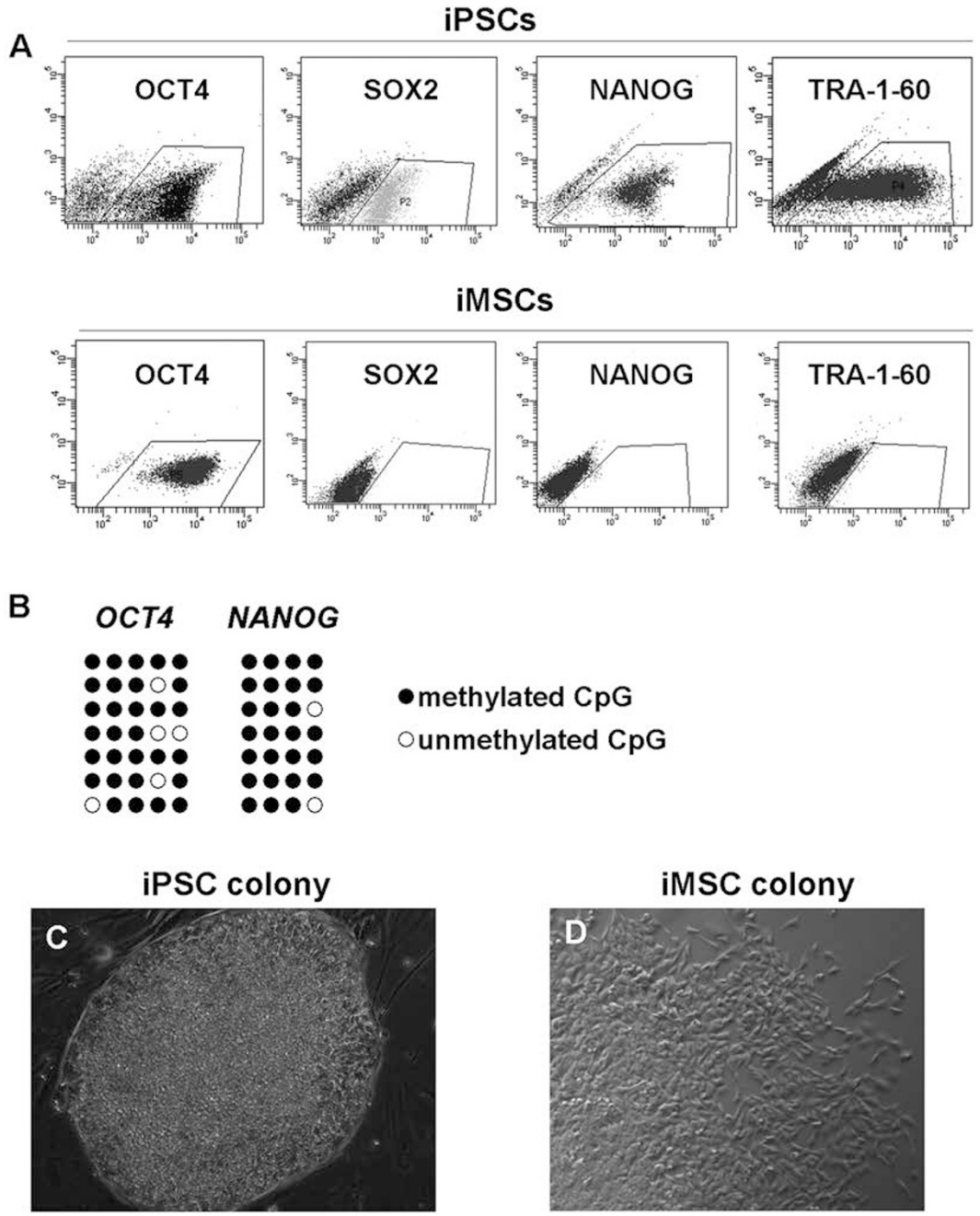

Figure 2 Reprogramming of CB-CD34$^+$ cells into iMSCs bypasses the pluripotent state. **(A)** Flow cytometry plots show that OCT4, but not other iPSC markers such as SOX2, NANOG and TRA-1-60, is expressed in Lenti iMSCs at 1 month after transduction. As positive controls, iPSCs express OCT4, SOX2, NANOG and TRA-1-60. **(B)** Bisulfite sequencing shows that *OCT4* and *NANOG* promoters remain hypermethylated in Lenti iMSCs after 2 months of culture. **(C)** A typical colony of iPSCs generated with OCT4 and SOX2. **(D)** A colony of iMSCs formed in iPSC culture conditions. OCT4-transduced CB-CD34$^+$ cells did not form iPSC-like colonies even after 1 month of culture in iPSC medium.

MSCs (Figure 3A-3C). A previous study shows that ectopic expression of OCT4 blocks the differentiation of epithelial progenitors [27]. We thus hypothesized that a high level of OCT4 expression promotes self-renewal, but inhibits differentiation of iMSCs. As predicted, after knockdown (KD) of OCT4 by 80% with an shOCT4 lentiviral vector (Supplementary information, Figure S5), iMSCs differentiated into mature adipocytes, osteoblasts

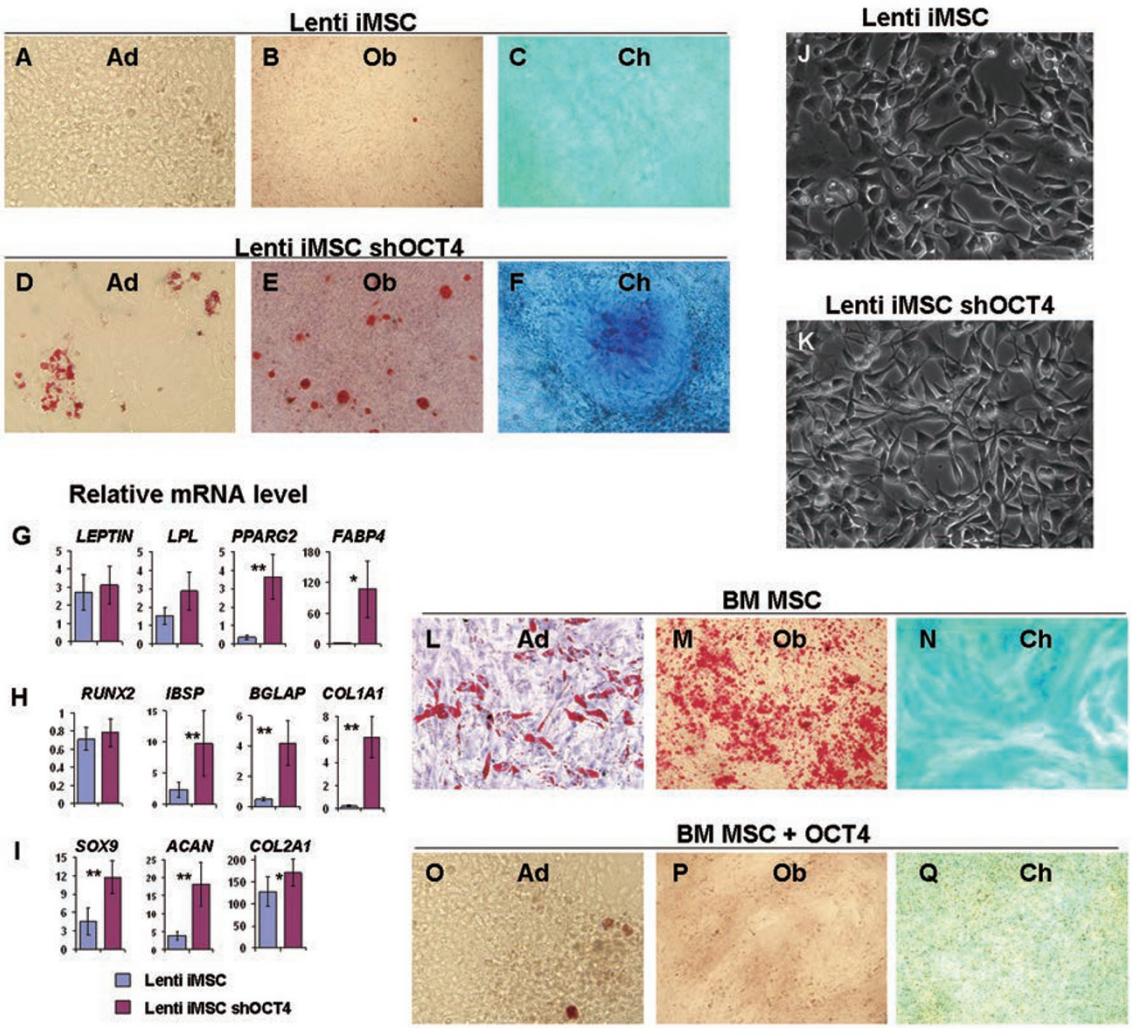

Figure 3 A high level of OCT4 expression in iMSCs inhibits the *in vitro* differentiation, whereas OCT4-KD allows for multilineage differentiation. **(A-F)** Lenti iMSCs do not differentiate into mature adipocytes (Ad), osteoblasts (Ob) or chondrocytes (Ch) under differentiation induction conditions for the indicated lineages **(A-C)**, whereas shRNA-mediated OCT4-KD allows for the terminal differentiation of Lenti iMSCs **(D-F)**. **(G-I)** RT-qPCR analyses of genes associated with adipogenic **(G**: *LEPTIN*, *PPARG2*, *LPL* and *FABP4*); osteoblastic (**H**: *RUNX2*, *IBSP*, osteocalcin (*BGLAP*) and *COL1A1*) and chondrogenic (**I**: *SOX9*, aggrecan (*ACAN*) and *COL2A1*) differentiation before or after OCT4-KD. mRNA expression levels were normalized to levels in the BM-MSC control. $^{**}P < 0.01$, $^{*}P < 0.05$. n = 10-20. Error bars indicate SEM. **(J)** Typical morphology of Lenti iMSCs at 1 month after OCT4 transduction. **(K)** Typical morphology of Lenti iMSCs at 2 weeks after OCT4-KD. **(L-N)** Images of *in vitro* differentiation of BM-MSC to Ad, Ob or Ch. **(O-Q)** Differentiation of BM-MSCs was blocked after Lenti-OCT4 transduction. Red stained are oil droplets in **D** and **L**, and bone nodules in **E** and **M**. Mucopolysaccharides secreted by chondrocytes are stained blue in **F** and **N**.

and chondrocytes (Figure 3D-3F). To quantitate the effects of OCT4-KD on MSC differentiation, we conducted real-time RT-PCR analyses. The results showed that OCT4-KD leads to significant upregulation of a majority of genes expressed specifically during adipocytic (Figure 3G), osteoblastic (Figure 3H) and chondrocytic (Figure 3I) differentiation. Of interest, OCT4-KD neither affected the long-term MSC proliferation potential, nor the expression of MSC markers (Supplementary information, Figure S6). We also observed that OCT4-KD leads to appreciable changes in morphology: Lenti iMSCs-expressing shOCT4 became more spindle-like compared with regular Lenti iMSCs (Figure 3J and 3K). To further evaluate the roles of OCT4 in MSC differentiation, we transduced BM-MSCs with OCT4. As expected, OCT4 overexpression in BM-MSCs led to differentiation failure (Figure 3L-3Q). Taken together, these data demonstrate that a high level of OCT4 blocks MSC differentiation,

and a reduction of OCT4 expression allows for multilineage differentiation.

Generation of integration-free iMSCs with an episomal vector

As a high level of constitutively expressed OCT4 inhibits iMSC differentiation and the use of integrating viral vector may limit the potential clinical applications, we attempted to reprogram CB-CD34$^+$ cells into iMSCs by a transient OCT4 overexpression with a non-integrating episomal vector (EV) [25, 28]. After nucleofection of CB-CD34$^+$ cells with EV SFFV-OCT4 plasmid DNA, we successfully generated iMSCs in 2 weeks, which we hereafter term as EV iMSCs for brevity. After 1 month of culture, OCT4 expression in EV iMSC decreased to baseline levels as observed in BM-MSCs (Supplementary information, Figure S5). EV iMSCs and BM-MSCs were morphologically identical (Figure 4A and 4B). In addition, EV iMSCs did not differ from regular MSCs in the expression of typical MSC markers (Supplementary information, Figure S7).

We next tested the *in vitro* differentiation potential of EV iMSCs in comparison with BM-MSCs. EV iMSCs fully differentiated into adipocytes, osteoblasts and chondrocytes, with the similar differentiation potentials as BM-MSCs (Figures 3L-3N, 4C-4E and Supplementary information, Figure S8). Further, results from RT-qPCR analyses showed similar expression levels for a majority of lineage-associated genes in adipocytes, osteoblasts and chondrocytes differentiated from EV iMSCs as compared to those differentiated from BM-MSCs (Figure 4F-4H). Of interest, the expression of *SOX9*, *ACAN* and *COL2A1* appeared to be higher in chondrocyte cultures of EV iMSCs than those of BM-MSCs. These data suggest that EV iMSCs are similar to BM-MSCs in the *in vitro* multilineage differentiation potency.

In vivo functionality of iMSCs

To evaluate the potential for clinical application of iMSCs, we further investigated the *in vivo* functionality of EV iMSCs. Cells were transduced with GFP to facilitate the analyses of human cells in mice. HA-TCP bone graft substitute blocks loaded with iMSCs were subcutaneously implanted in nude mice. Analyses of the implants 2-3 months later showed that iMSCs differentiated into bone tissue, connective fibers and adipose tissue in all 10 animals, and into skeletal muscle fibers in the majority of the implants (Figure 5A-5D). Immunohistological staining of GFP confirmed that the differentiated tissues were derived from human EV iMSCs (Figure 5E). Of interest, the implanted BM-MSCs differentiated into bone tissue, connective fibers and adipose tissue but not skeletal muscle fibers (Supplementary information, Figure S9). These data suggest that iMSCs may hold a functional advantage in promoting muscle regeneration.

Long-term proliferation and self-renewal of multipotent iMSCs depend on a low level of ectopic OCT4 expression

Primary adult human BM-MSCs display slowed proliferation after ~1 month in culture, and eventually stop growing and lose multilineage differentiation potential. We thus tested the *in vitro* proliferative potential of EV iMSCs. EV iMSCs showed an enhanced *in vitro* proliferative capacity compared with BM-MSCs — more than 100-fold more MSCs can be generated from the CB by transient OCT4 transfection than from the same volume of BM at 6 weeks after initiation of *in vitro* culture (Figure 6A). After ~15 passages in culture, EV iMSCs discontinued cell division and manifested the typical morphology of aged MSCs (Figure 6B).

Together with the observation of an unrestricted proliferative potential of Lenti iMSCs, we hypothesized that a low level of OCT4 expression may allow for long-term iMSC proliferation without blocking differentiation. To test this hypothesis, we selected a very weak promoter, the Sca1 promoter, which drives OCT4 expression at ~5% of the level in Lenti iMSCs or iPSCs (Supplementary information, Figure S5). After transducing EV iMSCs with Lenti Sca1-OCT4, these cells can be cultured for more than 30 passages, with a doubling time of ~40 h. In addition, Sca1-OCT4 iMSCs at passage 30 were still morphologically indistinguishable from BM-MSCs at earlier passages (Figure 6C). In addition, Sca1-OCT4 iMSCs readily differentiate into adipocytes, osteoblasts and chondrocytes in induction cultures (data not shown), suggesting that maintaining a low level of OCT4 expression in iMSCs allows for long-term proliferation, yet does not affect the *in vitro* multilineage differentiation potential of these cells.

Generation of iMSCs from adult human peripheral blood CD34$^+$ cells

Our findings with fetal blood prompted us to test whether OCT4 can also reprogram adult human peripheral blood (PB) cells into iMSCs. After transduction of PB-CD34$^+$ cells with Lenti SFFV-OCT4, iMSC colonies were formed within 1 week. The reprogramming of PB- and CB-CD34$^+$ cells was equally efficient. CHIR also increased the reprogramming efficiency of PB-CD34$^+$ cells from 3% to 15% (Figure 7A and 7B). In addition, PB-Lenti iMSCs were morphologically and phenotypically identical to CB-Lenti iMSCs (Figure 7C vs Figure 3J, and data not shown). These data suggest that OCT4 can reprogram both fetal and adult human hematopoietic

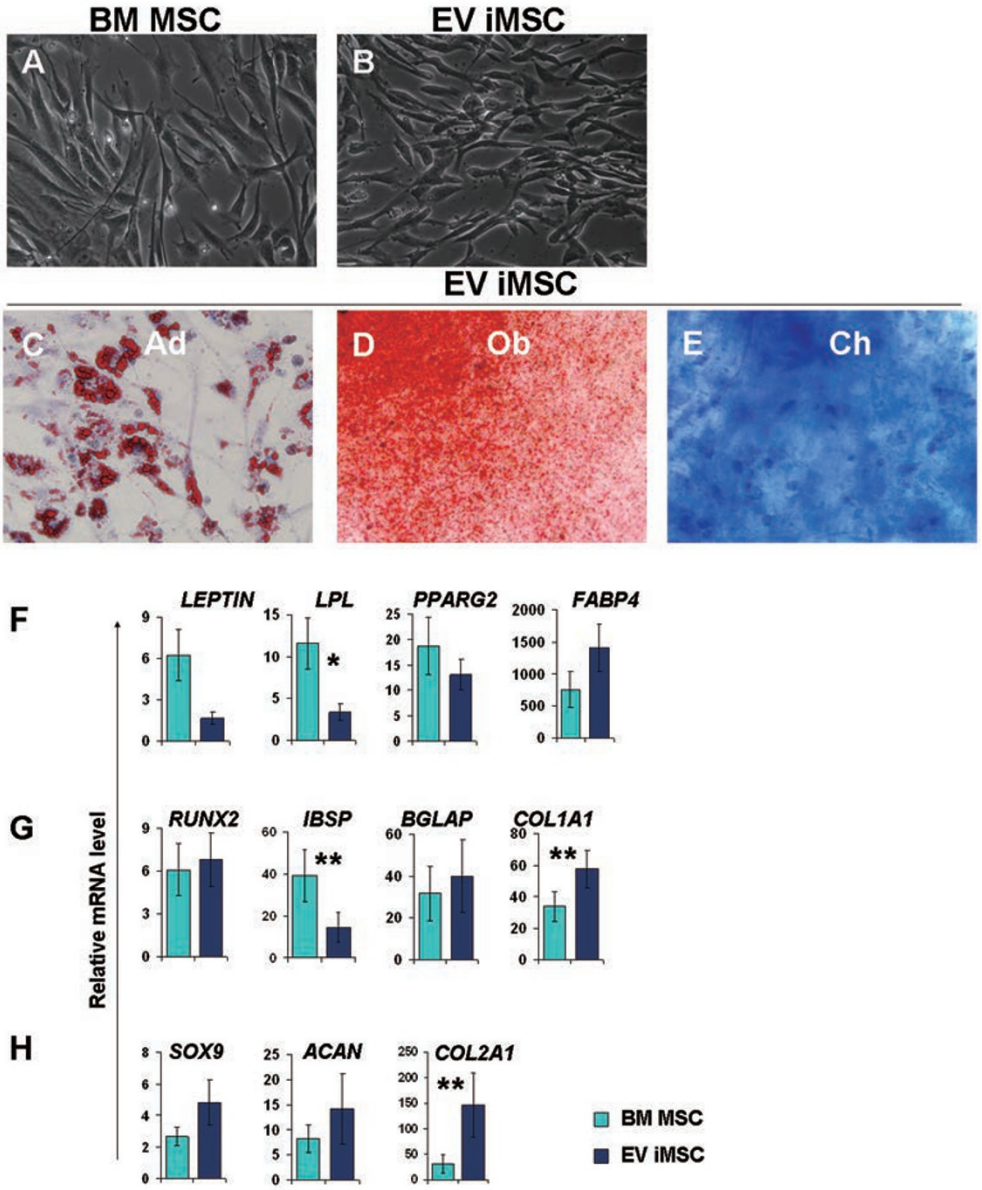

Figure 4 *In vitro* multilineage differentiation capacity of integration-free episomal iMSCs. **(A)** Typical morphology of BM-MSCs at passage 5. **(B)** Typical morphology of EV iMSCs at passage 5. BM-MNCs and EV iMSCs are morphologically indistinguishable. **(C**-**E)** iMSCs generated with episomal vector EV SFFV-OCT4 robustly differentiated into mature adipocytes (Ad) with oil droplets (red), osteoblasts (Ob) that form bone nodules (red) or chondrocytes (Ch) that secrete mucopolysaccharides (blue) after 3 weeks of induction culture. **(F)** RT-qPCR analyses of genes associated with adipogenic differentiation *LEPTIN*, *LPL*, *PPARG2* and *FABP4*. **(G)** RT-qPCR analyses of genes associated with osteoblastic differentiation *RUNX2*, *IBSP*, *BGLAP* and *COL1A1*. **(H)** RT-qPCR analyses of genes associated with chondrogenic differentiation *SOX9*, *ACAN* and *COL2A1*. The mRNA expression levels in **F**-**H** are normalized to the levels in BM-MSCs before the induction of differentiation. $^{**}P < 0.01$, $^{*}P < 0.05$. n = 10-20. Error bars indicate SEM.

cells into iMSCs at a similar efficiency.

Discussion

Here, we report that a single transcription factor, OCT4, allows for rapid and efficient reprogramming of human $CD34^{+}$ cells from either CB or adult PB directly into iMSCs. The ability to reprogram blood cells into self-renewable iMSCs at an unprecedented efficiency has important implications for regenerative medicine. Although MSCs have been isolated from many sources [10], our approach for generating iMSCs from the pa-

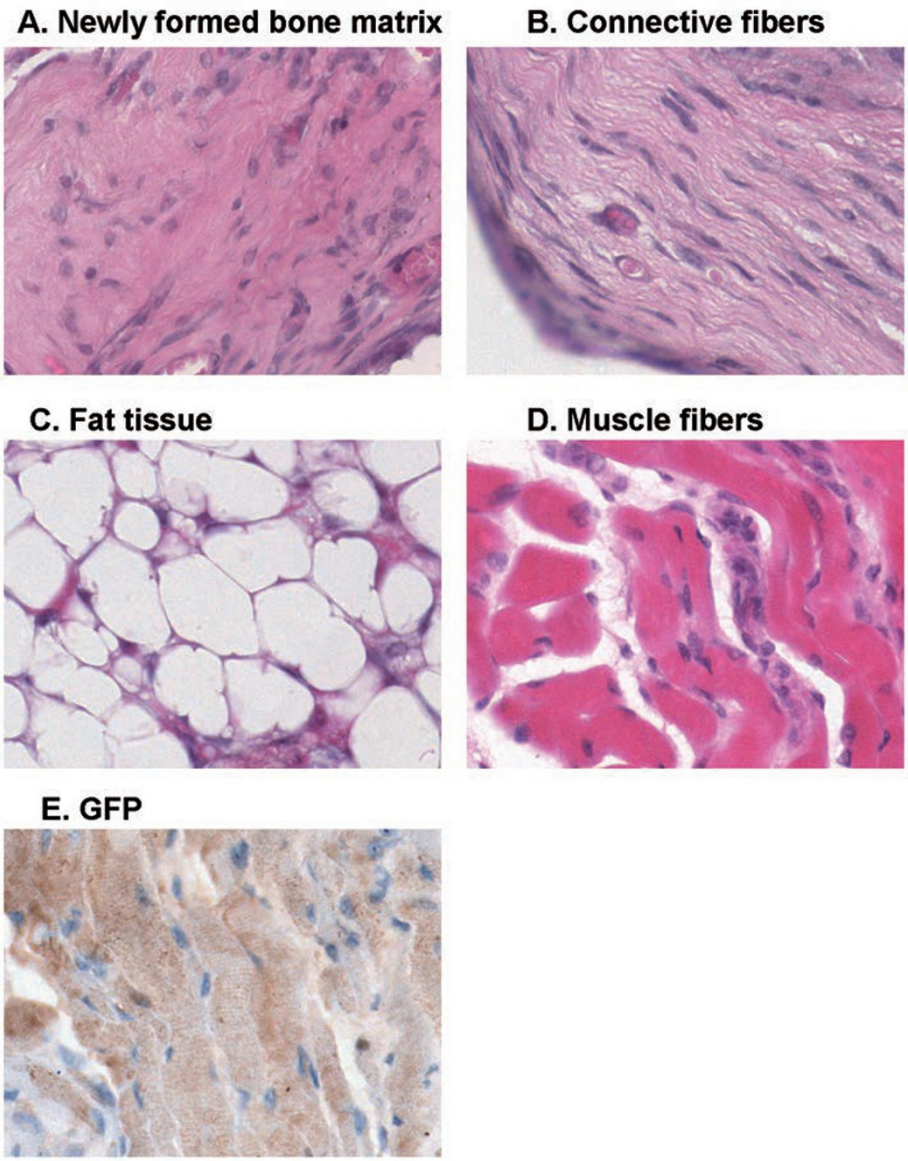

Figure 5 *In vivo* multilineage differentiation capacity of iMSCs. Two to three months after subcutaneous implantation of 1 × 10^6 EV iMSCs in HA-TCP blocks to nude mice, the implants were harvested for microsectioning and H&E staining analyses**. (A)** Newly formed bone matrix derived from the implanted iMSCs (400×). Bone matrix was formed in all of the implants (*n* = 10). **(B)** Connective tissues derived from the implanted iMSCs (400×). Connective tissue was formed in all the implants (*n* = 10). **(C)** Adipose tissue derived from implanted iMSCs (400×). Adipose tissue was formed in all the implants (*n* = 10). **(D)** Muscle fibers differentiated from the implanted iMSCs (400×). Muscle fibers were found in most of the implants (*n* = 10). **(E)** The expression of GFP demonstrates that cells are differentiated from human GFP-transduced EV iMSCs (400×). Brown colored tissues are stained GFP^+ cells.

tient's own blood cells should find its applications in the treatment of diseases such as arthritis and muscular dystrophy. The iMSCs are multipotent, being able to differentiate into different types of MSC progenies both *in vitro* and *in vivo*, and are not tumorigenic. In addition, with the use of an episomal vector, integration-free iMSCs can be generated. We also demonstrate a dosage effect of OCT4: a high level of OCT4 is required for efficient reprogramming, but blocks *in vitro* multilineage differentiation, whereas a low level of OCT4 promotes long-term self-renewal and proliferation but does not affect differentiation of iMSCs.

Due to the limited proliferative potential of MSCs derived from adult bone marrow or adipose tissue, many

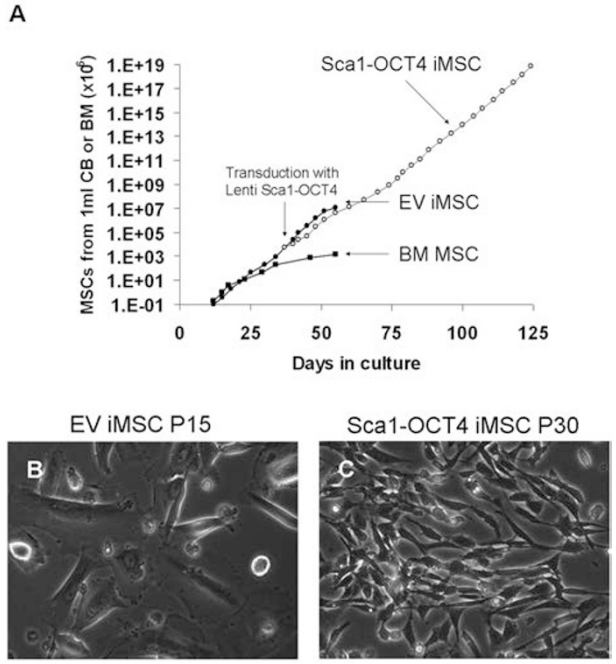

Figure 6 Integration-free EV iMSCs have greater proliferative potential than BM-MSCs and a low level of OCT4 expression allows for long-term expansion of iMSCs. **(A)** Numbers of MSCs generated from 1 ml BM by regular culture vs those from 1 ml CB by OCT4-mediated direct reprogramming. Integration-free EV iMSCs were generated by nucleofection of human CB-CD34$^+$ with the EV SFFV-OCT4 plasmid. 1 ml whole BM and CB-CD34$^+$ cells (1×10^5) from 1 ml CB were used in this experiment. Total MSCs were calculated by multiplying the numbers of MSCs with splitting factors of each passage. Sca1-OCT4 iMSCs were generated by transduction of EV iMSCs with Lenti Sca1-OCT4, in which the Sca1 promoter drives low-level OCT4 expression. Data shown are one representative result of 3 experiments with similar trends for *ex vivo* expansion of BM-MSCs, EV iMSCs and Sca1-OCT4 iMSCs. **(B)** Senescence morphology of EV iMSCs after 15 passages in culture. **(C)** Typical morphology of Sca1-OCT4 iMSCs after 30 passages in culture. After long-term *in vitro* culture, Sca1-OCT4 iMSCs still morphologically resemble BM-MSCs at low passages.

investigators have focused on the generation of MSCs from iPSCs. Earlier reports have shown that iPSC-MSCs are superior to adult MSCs in proliferative capacity and exhibit better or similar therapeutic effects in treating limb ischemia or allergic airway diseases, and promoting the ectopic formation of vascularized bone [11, 29-31]. The iMSC approach sidesteps the need for iPSC generation, and thus shortens the time required for generating large quantities of patient-specific MSCs from several months to several weeks, and lowers or even abrogates the risk of teratoma formation. We also demonstrate that iMSCs can differentiate to generate skeletal muscle, pointing to their potential applications in treating muscular disorders.

OCT4 is a master transcription factor that helps to maintain the pluripotency of embryonic stem cells and plays a pivotal role in the generation of iPSCs [32-34]. However, whether OCT4 is expressed in somatic stem cells like MSCs is controversial. Many earlier reports of OCT4 expression in somatic stem cells are likely due to artifacts caused by background noises and the expression of *OCT4* pseudogenes [35-36]. In addition, conditional knockout studies in mice demonstrate that OCT4 is functionally dispensable in self-renewal and differentiation of adult BM-MSCs [37]. However, the observation that OCT4 is not required for *in vivo* self-renewal of MSCs does not necessarily argue against the expression of OCT4 in MSCs during *ex vivo* culture and its potential effects on the functionality of MSCs. Recent reports have provided evidence that OCT4 expression is higher in MSCs at early passages compared with MSCs at late passages [38-39]. They also found that OCT4-KD in MSCs decreases the proliferation potential and enhances spontaneous differentiation of MSCs, whereas OCT4 overexpression in MSCs increases proliferation and sup-

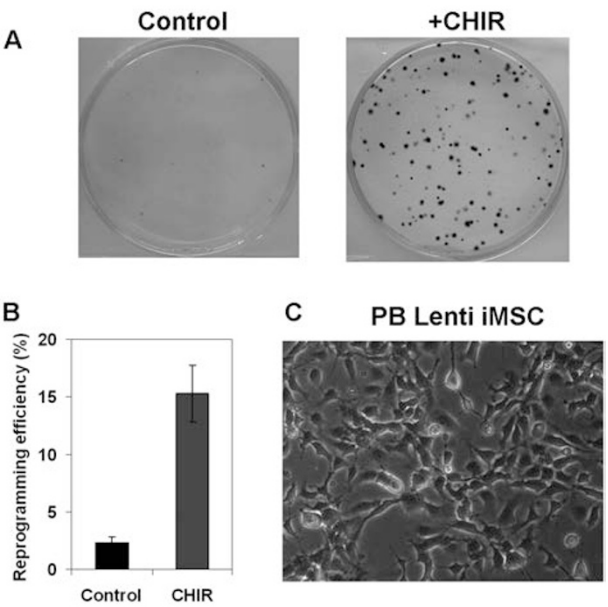

Figure 7 Efficient reprogramming of adult PB-CD34$^+$ cells into iMSCs. **(A)** MSC-like colonies formed from 1 000 OCT4-transduced PB-CD34$^+$ cells in the absence (control) or presence of CHIR99021 (+CHIR) after 9 days of culture in the MSC medium. **(B)** CHIR substantially increased the reprogramming efficiency from adult PB-CD34$^+$ cells into iMSCs (n = 3, P < 0.01). Error bars indicate SEM. **(C)** Typical morphology of PB-Lenti iMSCs at 1 month after OCT4 transduction.

presses spontaneous differentiation [39]. These data suggest an important role of OCT4 in maintaining the self-renewal of MSCs. This conclusion is further supported by a transgenic mouse study showing that ectopic OCT4 expression blocks the differentiation of epithelial progenitors [27]. Consistent with these observations, we show that a high level of ectopic OCT4 expression promotes long-term proliferation but inhibits iMSC differentiation, and that when OCT4 expression drops to baseline levels, iMSCs can initiate differentiation and eventually undergo senescence.

The use of OCT4 for iMSC generation is likely a safe approach due to several reasons. First, OCT4 expression is detected in germline tumors, but rarely identified in somatic tumors [40-41]. Second, although the inducible expression of OCT4 induces dysplasia in epithelial tissues, withdrawal of the induction stimulus leads to a complete reversal of the tumor-like phenotype. In addition, no mesenchymal tumor was observed in the OCT4 transgenic mouse model [27]. Third, iMSCs cultured in iPSC conditions do not form iPSC colonies, thus it is unlikely that iMSCs will induce teratoma formation after transplantation. In support of this notion, injection of Lenti iMSCs that express a high level of OCT4 does not induce tumors in immunodeficient mice. In contrast, coexpression of MYC in iMSCs did induce tumor formation (data not shown). Fourth, OCT4-generated iMSCs manifest a normal karyotype even after long-term culture, suggesting that ectopic OCT4 expression does not induce genomic abnormalities. In comparison, when MYC together with OCT4 was used for iMSC generation, chromosomal aneuploidies were observed (data not shown). Fifth, decreasing OCT4 expression to 5%-10% of the level expressed in iPSCs does not affect long-term self-renewal and expansion of iMSCs. A low level of OCT4 expression is sufficient to maintain iMSC self-renewal, but does not affect its multilineage differentiation, thus is unlikely to pose any significant risk in clinical use.

We provide compelling evidence that MSCs can be directly reprogrammed from hematopoietic cells. Although vascular and other endothelial cells also express CD34, the source cells we used for reprogramming also express CD45 (Supplementary information, Figure S2A and data not shown), arguing against the possibility that iMSCs are derived from endothelial cells. The time-lapse video also demonstrates the morphological changes from hematopoietic cells to fibroblast-like cells (Supplementary information, Video S2). In addition, single-cell cloning experiment rules out the possibility that OCT4 overexpression expands contaminated MSCs in $CD34^+$ cells (Supplementary information, Figure S4). Due to the unprecedented high reprogramming efficiency of 16%, our findings cannot be explained by the proliferation of trace amount of endothelial cells, MSCs or other types of unknown cells that express CD34.

Many *in vitro* studies used integrating-viral vectors for direct cell reprogramming. Although silencing of the viral vector was observed in some studies [14], reactivation of the reprogramming factor may still pose a long-term risk after cell transplantation. Here, we show that OCT4 expression via a nonintegrating episomal vector is sufficient to induce direct reprogramming of $CD34^+$ cells into iMSCS, making this approach one step closer to clinical therapy.

The capacity for long-term undifferentiated proliferation of iMSCs in the presence of low levels of OCT4 expression has important implications for MSC-based therapy. A low level of OCT4 expression in iMSCs does not affect iMSC terminal differentiation. This provides the possibility of a safe autologous MSC-based therapy, as one could select a clone with lentiviral vector integration at the "genomic safe harbors" for expansion and therapy. In this study, we used a weak promoter (Sca1) to drive the low-level OCT4 expression in EV iMSCs. Alternatively, identification of small molecules or microRNAs that can turn on OCT4 expression in MSCs may be useful for promoting the self-renewal of iMSCs and even adult MSCs.

Our study represents the first report that somatic stem cells can be efficiently reprogrammed from hematopoietic cells in adult human peripheral blood. Direct conversion of fibroblasts into cells of clinical interests has been reported by many groups. Due to the obvious advantages of using blood cells compared with fibroblasts derived from skin biopsy, our findings provide a foundation for further investigations into the possibility of direct conversion of blood cells into other cell types such as neural stem cells [14], cardiomyocytes [16-17] and hepatocytes [18-19]. Alternatively, due to the biological similarities between fibroblasts and MSCs [42-43], iMSCs may also constitute a cell source comparable to fibroblasts for generating cells of clinical interest.

Materials and Methods

CB and PB $CD34^+$ cells

The use of human CB was approved by the Institutional Review Board of Loma Linda University and written informed consent was obtained from all participants. $CD34^+$ cells were purified with a CD34 Microbead Kit (Miltenyi Biotec, Auburn, CA, USA). Mobilized PB $CD34^+$ cells were purchased from AllCells LLC (Emeryville, CA, USA).

Lentiviral vectors and episomal vector

In conducting work involving the use of recombinant DNA, the investigators adhered to the current version of the National Institute of Health (NIH) Guidelines for Research Involving Recombinant DNA Molecules. The lentiviral vectors used in this study have been described previously [25]. In these vectors, the SFFV, EF1, PGK or Sca1 promoters were used to drive OCT4 expression at different levels in $CD34^+$ cells [25]. The details of lentiviral vector packaging and titering have been published elsewhere [44]. In brief, the calcium precipitation method was used for generating lentiviral vector. After 100-fold concentration by ultracentrifugation, the biological titers of vectors were determined by transducing HT1080 cells. For generating integration-free iMSCs, OCT4 was subcloned into our improved ENBA/oriP-based episomal vector, in which the SFFV promoter and Wpre element were included to drive high-level transgene expression in hematopoietic cells [25]. For OCT4-KD, the shOCT4 lentiviral vector (catalog no: RHS3979-9573664) was purchased from Thermo Scientific Open Biosystems.

BM-MSCs

Human BM samples were purchased from AllCells, LLC. To generate BM-MSCs, whole BM was cultured in human fibronectin (BD Biosciences, San Jose, CA, USA)-precoated culture plates with the Mesenchymal Stem Cell (MSC) Medium Kit from Applied Biological Materials Inc. (ABM; Richmond, BC, Canada). The cultures were kept at 37 °C with 5% CO_2 in a water-jacketed incubator. Cells were cultured under hypoxia by placing culture plates in Hypoxia Chambers (Stemcell Technologies, Inc., Vancouver, BC, Canada) that were flushed with mixed air composed of 92% N_2/3% O_2/5% CO_2. Culture medium was changed every 1-2 days. Approximately 10 days later, when MSC-like colonies appeared, cells were passaged every 3-5 days after treatment with accutase (Innovative Cell Technologies, Inc., San Diego, CA, USA) for 5 min. BM-MSCs at passages 3-6 were used in this study as a positive control. Some BM-MSCs were purchased from ABM.

iMSC generation with lentiviral or episomal vectors

To generate Lenti iMSCs, thawed human CB-$CD34^+$ cells or G-CSF-mobilized PB-$CD34^+$ cells (AllCells) were cultured in HSC culture medium: Iscove's modified Dulbecco's medium (IMDM; Life Technologies, Grand Island, NY, USA)/10% fetal bovine serum (FBS; ABM) supplemented with TPO, SCF and Flt3 ligand (FL) each at 100 ng/ml, and G-CSF and IL-3 at 10 ng/ml [45]. Cytokines were purchased from ProSpec (East Brunswick, NJ, USA). $CD34^+$ cells were cultured for 2 days before transduction. For transduction, cells were inoculated in fibronectin fragment CH-296 (RetroNectin; Takara Bio Inc., Shiga, Japan)-pretreated non-TC-well plates and transduced with Lenti SFFV-OCT4 at a multiplicity of infection (MOI) of 2-5 for 4-5 h. A second transduction was performed the next day. To determine transduction efficiency, one well of cells were transduced with Lenti SFFV-GFP. After 2 transductions, 80%-95% cells were GFP^+. OCT4-transduced cells were cultured in MSC medium. 4 to 6 days later, when $CD34^+$ cells were morphologically transforming into MSC-like colonies, cells were split at a ratio of 4-6:1 to human fibronectin-treated non-TC plates. In some cultures, GSK3 inhibitor CHIR99021 (ABM) was also added at a final concentration of 3 μM. For long-term culture, cells were passaged every 2-3 days and cultures were maintained in hypoxia.

To generate integration-free iMSCs, fresh or thawed 1×10^6 CB-$CD34^+$ cells were cultured in IMDM/10% FBS supplemented with TPO, SCF and FL at 100 ng/ml. 1 to 2 days later, cells were harvested for nucleofection with a total of 10 μg EV SFFV-OCT4 plasmid DNA. Human CD34 Cell Nucleofector® Kit (Lonza, Koln, Germany) was used. Nucleofection was performed with Amaxa Nucleofector II using program U-008. Immediately after nucleofection, cells were suspended in HSC medium and gently transferred to a CH-296-pretreated non-TC well plate and spun down for 5 min at 400× *g* to improve cell survival. Starting the next day, MSC medium was added to the culture wells. At 1-2 weeks after nucleofection, when MSC-like colonies were formed, cells were passaged to human fibronectin-treated non-TC 6-well plates. In the first 2 weeks of culture, CHIR99021 (ABM) was also added at a final concentration of 3 μM. For long-term culture, episomal iMSCs were passaged every 2-4 days and cultures were maintained in hypoxia.

Single $CD34^+$ cell cloning and iMSC generation

To rule out the possibility that some MSCs are carried along during CD34 cell enrichment, we conducted single cell cloning. Single CB-$CD34^+$ cells were cultured in four U-bottomed 96-well plates in IMDM/10% FBS supplemented with TPO, SCF and FL at 100 ng/ml, and IL-3 and G-CSF at 10 ng/ml. Ten days later, colonies with more than 100 cells were formed in ~10% wells. Twelve clones were randomly selected and transferred to a CH-296-pretreated non-TC 12-well plate. After overnight transduction with Lenti SFFV-OCT4, cells were cultured in a mixture of HSC medium and MSC medium at a 20:80 ratio. At 5 and 8 days after transduction, cultures were refreshed with MSC medium. CHIR99021 (ABM) was added throughout the culture. At 10 days after transduction, the culture plate was stained with crystal violet stain.

Calculation of reprogramming efficiency

To calculate transdifferentiation efficiency, 1000 Lenti SFFV-OCT4-transduced $CD34^+$ cells were seeded into CH-296-pretreated non-TC 6-well plates. HSC medium and MSC medium were added at a 20:80 ratio. In some wells, 3 μM CHIR99021 (ABM) was added to the medium. Five days later and every 2 days thereafter, the culture was refreshed with MSC medium. At 9 days after transdifferentiation of culture, the plate was stained with crystal violet stain and colonies were enumerated.

Cell imaging

Phase contrast pictures were taken using a Nikon converted microscope with a 10× objective. For time-lapse live cell imaging, $CD34^+$ cells were transduced with Lenti SFFV-OCT4 or GFP control vectors. One day after transduction, 1×10^4 cells were seeded in each well of a CH-296-pretreated non-TC 6-well plate. Cells were cultured in HSC medium or MSC medium supplemented with 3 μM CHIR99021. At day 4, culture medium was changed. Phase contrast pictures of cells in culture were taken every 2 h for 6 days in a BioStation CT (Nikon Instruments Inc.) at UCR (University of California Riverside) Stem Cell Center Core Facility. The pictures were edited and videos composed with ImageJ.

Flow cytometry

To phenotype iMSCs, cells were stained with hematopoietic markers CD14, CD34 and CD45, endothelial marker CD31, MSC markers CD29, CD44, CD73, CD90, CD105 and CD166, and

iPSC markers OCT4, SOX2, NANOG and TRA-1-60. All antibodies except otherwise specified were purchased from eBioscience, Inc. (San Diego, CA, USA). For staining of cell surface markers, CD14-FITC, CD29-APC (BD Biosciences), CD31-PE, CD34-PE, CD44-PE, CD45-FITC, CD73-APC, CD90-PE, CD105-APC, TRA-1-60-PE, CD166-PE (BioLegend, Inc., San Diego, CA, USA) cells were incubated with each antibody for 30 min at room temperature in FACS buffer in the dark. For intracellular staining, cells were fixed for 20 min at room temperature in a fixation buffer supplemented with 10% permeabilization buffer (eBioscience). After 2 washes with FACS buffer, cells were incubated with OCT4-PE, SOX2-FITC or NANOG-PE (BD Biosciences) for 2 h at room temperature in the dark. Following incubation, the samples were washed twice with FACS buffer supplemented with 10% permeabilization buffer. Flow cytometric analysis was performed using the FACS Aria II with a 488 nm laser (BD Biosciences).

In vitro differentiation of MSCs

For adipocytic differentiation, 1×10^5 iMSCs or BM-MSCs were seeded in each well of TC-treated 6-well plates. Adipocytic differentiation was induced with 1 μM dexamethasone (Sigma-Aldrich Corp, St Louis, MO, USA), 1 μM troglitazone (Sigma), 10 μg/ml insulin (Sigma), 0.5 mM isobutylxanthine (Sigma), 5 ng/ml of FGF2 (ABM) and 10% FBS in α-MEM (Life Technologies) with 1% penicillin/streptomycin (P/S). For osteoblastic differentiation, 2×10^5 cells were seeded in each well of TC-treated 6-well plates. Osteoblastic differentiation was induced with 0.1 μM dexamethasone (Sigma), 200 μM ascorbic acid (Sigma), 10 mM β-glycerol phosphate (Sigma), 10 ng/ml BMP2 (ABM), 10 ng/ml BMP4 (ABM) and 10% FBS in α-MEM. For chondrogenic differentiation, 4×10^5 cells were seeded in each well of TC-treated 6-well plates. Chondrogenic differentiation was induced in α-MEM/10% FBS/1% P/S supplemented with 0.1 μM dexamethasone, 200 μM ascorbic acid, 5.33 μg/ml linoleic acid, 0.35 mM L-proline, 10 ng/ml TGFβ3 (Stemgent, San Diego, CA, USA), 10 ng/ml TGFβ1 (ABM) and 1% ITS (insulin-transferrin-selenium; Life Technologies).

All cultures were maintained with 5% CO_2 in a water-jacketed incubator at 37 °C, and culture media were changed every 2-3 days. Three to four weeks after differentiation culture, cells were fixed in 10% neutral buffered formalin for 15 min before staining. Adipocytes were stained with Oil Red O solution for 15 min. Oil Red O working solution was made by diluting Oil Red O stock solution with nanopure water at a 3:2 ratio. Oil Red O stock solution was made by dissolving 0.5 g of Oil Red O powder in 100 ml isopropanol with gentle heat and then filtered with a 5 μm syringe filter. After 15 min of incubation with 1 ml of Oil Red O working solution, the stain was washed out with 60% isopropanol. Bone nodule formation was evaluated by Alizarin Red staining. After formalin fixation, 1 ml of Alizarin Red staining solution was added for 5 min and the cells were washed with nanopure water. Alizarin Red staining solution was made by dissolving 2 g of Alizarin Red in 100 ml of nanopure water. The pH was adjusted to 4.3 with 10% ammonium hydroxide and then filtered with a 5 μm syringe filter. To stain mucopolysaccharides associated with chondrocytic differentiation, fixed cultures were stained with Alcian Blue staining solution for 30 min. The cultures were later washed in tap water for 2 min and then rinsed in nanopure water. Alcian Blue staining solution was prepared by dissolving 1 g of Alcian Blue in 100 ml of 3% acetic acid solution. The pH was adjusted to 2.5 using acetic acid.

RNA isolation and quantitative real-time RT-PCR

To induce *in vitro* multilineage differentiation of iMSCs and BM-MSC controls, cells were cultured in conditions detailed above. At 2 or 3 weeks after differentiation culture, cells were harvested using cell scrappers or by treating with trypsin (ABM). Total RNA was extracted with Trizol reagent and RNeasy kit (Qiagen, Inc., Valencia, CA, USA). Reverse transcription was performed using the EasyScript Plus cDNA Synthesis Kit (ABM), following the manufacturer's recommendations. Quantitative real-time RT-PCR (qPCR) was performed as previously described [44]. Expression of differentiation-associated genes at 2 or 3 weeks after induction of cultures were not significantly different, and thus were combined for analysis. Expression of *OCT4* and lineage-specific markers was normalized to the expression of *ACTB*. The sequences of primers for qPCR are as follows: ACTB forward, 5′-TCGTGCGTGACATTAAGGAG-3′; reverse, 5′-GGCAGCTCGTAGCTCTTCTC-3′; LEPTIN forward, 5′-GAAGACCACATCCACACACG-3′; reverse, 5′-AGCTCAGCCAGACCCATCTA-3′; LPL forward, 5′-ATTTGCCCTAAGGACCCC-3′; reverse, 5′-ATGACAGGTAGCCACGGAC-3′; PPARG2 forward, 5′-AGAAGCCTGCATTTCTGCAT-3′; reverse, 5′-TCAAAGGAGTGGGAGTGGTC-3′; FABP4 forward, 5′-TACTGGGCCAGGAATTTGAC-3′; reverse, 5′-GTGGAAGTGACGCCTTTCAT-3′; RUNX2 forward, 5′-TTTGCACTGGGTCATGTGTT-3′; reverse, 5′-TGGCTGCATTGAAAAGACTG-3′; BGLAP forward, 5′-TCACACTCCTCGCCCTATTG-3′; reverse, 5′-TCGCTGCCCTCCTGCTTG-3′; IBSP forward, 5′-GCAGTAGTGACTCATCCGAAGAA-3′; reverse, 5′-GCCTCAGAGTCTTCATCTTCATTC-3′; COL1A1 forward, 5′-GCCATCAAAGTCTTCTGC-3′; reverse, 5′-ATCCATCGGTCATGCTCT-3′; ACAN forward, 5′-CGCTACTCGCTGACCTTT-3′; reverse, 5′-GCTCATAGCCTGCTTCGT-3′; SOX9 forward, 5′-GACTTCCGCGACGTGGAC-3′; reverse, 5′-GTTGGGCGGCAGGTACTG-3′; COL2A1 forward, 5′-TCCCAGAACATCACCTACC-3′; reverse, 5′-AACCTGCTATTGCCCTCT-3′; OCT4 forward, 5′-CTTGCTGCAGAAGTGGGTGGAGGAA-3′; reverse, 5′-CTGCAGTGTGGGTTTCGGGCA-3′.

Tumor formation assay

The use of NOD/SCID/IL2RG$^{-/-}$ (NSG) immunodeficient mice for the tumor formation assay was approved by the Institutional Animal Care and Use Committee at Loma Linda University (LLU). In conducting research using animals, the investigators adhered to the Animal Welfare Act Regulations and other Federal statutes relating to animals and experiments involving animals, and the principles set forth in the current version of the Guide for Care and Use of Laboratory Animals, National Research Council. NSG mice were purchased from the Jackson Laboratory (Bar Harbor, MA, USA) and maintained at the LLU animal facility. To facilitate detection of human cells in mice, iMSCs were transduced with GFP. 1×10^6 Lenti iMSCs were harvested by Accutase digestion, washed with culture medium and re-suspended in 200 μl MSC medium-diluted (1:1) Matrigel solution (BD Biosciences). Cells were then injected into the subcutaneous tissue of NSG mice. As a positive control, clumps of ~1×10^6 iPSCs in Matrigel were injected subcutaneously. In some mice, 2×10^6 Lenti iMSCs were also injected via tail vein. Two to three months after transplantation, mice were euthanized to examine the presence of solid tumor in multiple organs. To detect the presence of leukemia, BM cells were harvested for FACS analysis.

Bisulphite sequencing

Bisulphite sequencing of genomic DNA from iMSCs was used to assess methylation status of *OCT4* and *NANOG* promoter. Genomic DNA was purified with a DNeasy Kit (Qiagen, Inc.). The conversion of unmethylated cytosines to uracil was carried out using EZ DNA Methylation-Gold Kit (ZYMO Research Corp., Irvine, CA, USA). The experimental procedure was detailed in a previous publication [25].

Karyotyping and G-banding

Giemsa (GTG)-banding chromosome analysis was carried out in the LLU Radiation Research Laboratories. Standard DNA spectral karyotyping procedures were followed and a HiSKY Complete Cytogenetic System was used (Applied Spectral Imaging, Inc. Vista, CA, USA). Ten metaphases were analyzed and karyotyped. The data were interpreted by a board-certified cytogenetic technologist.

In vivo MSC differentiation assay

Experimental procedures were approved by the Animal Care and Use Committee of the Chinese University of Hong Kong. 1 × 10^6 GFP-transduced EV iMSCs or BM-MSCs were absorbed into the porous Skelite® resorbable HA-TCP bone graft substitute blocks (size: 0.4 × 0.4 × 0.4 cm) for 2 h to allow cell attachment. The cells-HA/TCP block was then implanted subcutaneously into the dorsal side of female nude mice. At 8-12 weeks after implantation, the implants were harvested and fixed with 10% neutral buffered formalin, decalcified with 9% formic acid for 2-3 weeks and embedded in paraffin for histological examination. The 5-μm microsectioning slides were deparaffinized and rehydrated, and endogenous peroxidase was quenched by rinsing in 3% hydrogen peroxide in methanol for 20 min. Hematoxylin and Eosin (H&E) staining was performed using standard protocol. To identify progeny of human GFP-expressing iMSCs, we conducted immunohistological staining against GFP. After washing in PBS, antigen retrieval was carried out in 10 mM citrate buffer at 37 °C for 10 min, and followed by 3 washes in PBS. The samples were blocked with 10% goat serum in 1% BSA/PBS for 1 h at room temperature. Primary antibody against GFP (1:50; Santa Cruz Biotechnology, Inc., Santa Cruz, CA, USA) was added and the blocking solution was used as negative control. After overnight incubation at 4 ºC, the samples were washed in PBS 3 times and incubated with HRP-conjugated anti-rabbit secondary antibody (1:200; Santa Cruz Biotechnology) for 1 h at room temperature. After PBS washing, peroxidase substrate DAB (Dako, Carpinteria, CA, USA) was used for color development (1 min for GFP). The samples were immersed in distilled water, dehydrated and cleared before being mounted with DPX.

Statistical analysis

Data are presented as mean ± standard error of the mean (SEM). Mann-Whitney *U* test was performed for RT-qPCR data and two-tailed Student's *t*-test was performed for other comparisons. $P < 0.05$ was considered statistically significant.

Acknowledgments

We thank Drs Prudence Talbot and Duncan Liew at UCR Stem Cell Center for help with the time-lapse imaging and Linda Ritter for technical support in karyotype analysis. This work was supported by the Loma Linda University Department of Medicine (XBZ), a Loma Linda University GRASP Award (XBZ), USAMRAA Concept Award W81XWH-11-1-0607 (XBZ), the Division of Anatomy, the Department of Basic Sciences, the Center for Health Disparities and Molecular Medicine at Loma Linda University (KJP and RJS) and Radiation Research Laboratories in the Department of Radiation Medicine at Loma Linda University (DSG). This work was also supported by the Telemedicine and Advanced Technology Research Center (TATRC) at the US Army Medical Research and Materiel Command (USAMRMC) under grant no. W81XWH-12-1-0023 (DJB). We thank National Natural Science Foundation of China (30872635 and 81172177) and Hong Kong Government Research Grant Council General Research Fund (CUHK471110) for financial support (GL). The work was also supported in part by National Basic Research Program of China to GL (973 Program 2012CB518105).

References

1 Pittenger MF, Mackay AM, Beck SC, *et al.* Multilineage potential of adult human mesenchymal stem cells. *Science* 1999; **284**:143-147.
2 Chamberlain JR, Schwarze U, Wang PR, *et al.* Gene targeting in stem cells from individuals with osteogenesis imperfecta. *Science* 2004; **303**:1198-1201.
3 Uematsu K, Hattori K, Ishimoto Y, *et al.* Cartilage regeneration using mesenchymal stem cells and a three-dimensional poly-lactic-glycolic acid (PLGA) scaffold. *Biomaterials* 2005; **26**:4273-4279.
4 Young RG, Butler DL, Weber W, Caplan AI, Gordon SL, Fink DJ. Use of mesenchymal stem cells in a collagen matrix for achilles tendon repair. *J Orthop Res* 1998; **16**:406-413.
5 Fan H, Liu H, Wong EJW, Toh SL, Goh JCH. *In vivo* study of anterior cruciate ligament regeneration using mesenchymal stem cells and silk scaffold. *Biomaterials* 2008; **29**:3324-3337.
6 Le Blanc K, Frassoni F, Ball L, *et al.* Mesenchymal stem cells for treatment of steroid-resistant, severe, acute graft-versus-host disease: a phase II study. *Lancet*; **371**:1579-1586.
7 Dalal J, Gandy K, Domen J. Role of mesenchymal stem cell therapy in Crohn's disease. *Pediatr Res* 2012; **71**:445-451.
8 Tan J, Wu W, Xu X, *et al.* Induction therapy with autologous mesenchymal stem cells in living-related kidney transplants: a randomized controlled trial. *JAMA* 2012; **307**:1169-1177.
9 Domínguez-Bendala J, Lanzoni G, Inverardi L, Ricordi C. Concise review: mesenchymal stem cells for diabetes. *Stem Cells Transl Med* 2011; **1**:59-63.
10 Mosna F, Sensebe L, Krampera M. Human bone marrow and adipose tissue mesenchymal stem cells: a user's guide. *Stem Cells Dev* 2010; **19**:1449-1470.
11 Lian Q, Zhang Y, Zhang J, *et al.* Functional mesenchymal stem cells derived from human induced pluripotent stem cells attenuate limb ischemia in mice. *Circulation* 2010; **121**:1113-1123.
12 Deyle DR, Khan IF, Ren G, *et al.* Normal collagen and bone production by gene-targeted human osteogenesis imperfecta iPSCs. *Mol Ther* 2012; **20**:204-213.
13 Jung Y, Bauer G, Nolta JA. Concise review: induced pluripotent stem cell-derived mesenchymal stem cells: progress

toward safe clinical products. *Stem Cells* 2012; **30**:42-47.
14 Ring KL, Tong LM, Balestra ME, *et al.* Direct reprogramming of mouse and human fibroblasts into multipotent neural stem cells with a single factor. *Cell Stem Cell* 2012; **11**:100-109.
15 Han DW, Tapia N, Hermann A, *et al.* Direct reprogramming of fibroblasts into neural stem cells by defined factors. *Cell Stem Cell* 2012; **10**:465-472.
16 Song K, Nam YJ, Luo X, *et al.* Heart repair by reprogramming non-myocytes with cardiac transcription factors. *Nature* 2012; **485**:599-604.
17 Ieda M, Fu JD, Delgado-Olguin P, *et al.* Direct reprogramming of fibroblasts into functional cardiomyocytes by defined factors. *Cell* 2010; **142**:375-386.
18 Huang P, He Z, Ji S, *et al.* Induction of functional hepatocyte-like cells from mouse fibroblasts by defined factors. *Nature* 2011; **475**:386-389.
19 Sekiya S, Suzuki A. Direct conversion of mouse fibroblasts to hepatocyte-like cells by defined factors. *Nature* 2011; **475**:390-393.
20 Haase A, Olmer R, Schwanke K, *et al.* Generation of induced pluripotent stem cells from human cord blood. *Cell Stem Cell* 2009; **5**:434-441.
21 Giorgetti A, Montserrat N, Aasen T, *et al.* Generation of induced pluripotent stem cells from human cord blood using OCT4 and SOX2. *Cell Stem Cell* 2009; **5**:353-357.
22 Ye Z, Zhan H, Mali P, *et al.* Human-induced pluripotent stem cells from blood cells of healthy donors and patients with acquired blood disorders. *Blood* 2009; **114**:5473-5480.
23 Loh YH, Agarwal S, Park IH, *et al.* Generation of induced pluripotent stem cells from human blood. *Blood* 2009; **113**:5476-5479.
24 Giorgetti A, Marchetto MC, Li M, *et al.* Cord blood-derived neuronal cells by ectopic expression of Sox2 and c-Myc. *Proc Natl Acad Sci USA* 2012; **109**:12556-12561.
25 Meng X, Neises A, Su RJ, *et al.* Efficient reprogramming of human cord blood CD34+ cells into induced pluripotent stem cells with OCT4 and SOX2 alone. *Mol Ther* 2012; **20**:408-416.
26 Bieback K, Kern S, Kluter H, Eichler H. Critical parameters for the isolation of mesenchymal stem cells from umbilical cord blood. *Stem Cells* 2004; **22**:625-634.
27 Hochedlinger K, Yamada Y, Beard C, Jaenisch R. Ectopic expression of Oct-4 blocks progenitor-cell differentiation and causes dysplasia in epithelial tissues. *Cell* 2005; **121**:465-477.
28 Chou BK, Mali P, Huang X, *et al.* Efficient human iPS cell derivation by a non-integrating plasmid from blood cells with unique epigenetic and gene expression signatures. *Cell Res* 2011; **21**:518-529.
29 Sun YQ, Deng MX, He J, *et al.* Human pluripotent stem cell-derived mesenchymal stem cells prevent allergic airway inflammation in mice. *Stem Cells* 2012; **30**:2692-2699.
30 Fu QL, Chow YY, Sun SJ, *et al.* Mesenchymal stem cells derived from human induced pluripotent stem cells modulate T-cell phenotypes in allergic rhinitis. *Allergy* 2012; **67**:1215-1222.
31 Domev H, Amit M, Laevsky I, Dar A, Itskovitz-Eldor J. Efficient engineering of vascularized ectopic bone from human embryonic stem cell-derived mesenchymal stem cells. *Tissue Eng Part A* 2012; 18:2290-302.
32 Nichols J, Zevnik B, Anastassiadis K, *et al.* Formation of pluripotent stem cells in the mammalian embryo depends on the POU transcription factor OCT4. *Cell* 1998; **95**:379-391.
33 Boyer LA, Lee TI, Cole MF, *et al.* Core transcriptional regulatory circuitry in human embryonic stem cells. *Cell* 2005; **122**:947-956.
34 Takahashi K, Yamanaka S. Induction of pluripotent stem cells from mouse embryonic and adult fibroblast cultures by defined factors. *Cell* 2006; **126**:663-676.
35 Lengner CJ, Welstead GG, Jaenisch R. The pluripotency regulator OCT4: a role in somatic stem cells? *Cell Cycle* 2008; **7**:725-728.
36 Liedtke S, Enczmann J, Waclawczyk S, Wernet P, Kogler G. OCT4 and its pseudogenes confuse stem cell research. *Cell Stem Cell* 2007; **1**:364-366.
37 Lengner CJ, Camargo FD, Hochedlinger K, *et al.* OCT4 expression is not required for mouse somatic stem cell self-renewal. *Cell Stem Cell* 2007; **1**:403-415.
38 Greco SJ, Liu K, Rameshwar P. Functional similarities among genes regulated by OCT4 in human mesenchymal and embryonic stem cells. *Stem Cells* 2007; **25**:3143-3154.
39 Tsai CC, Su PF, Huang YF, Yew TL, Hung SC. OCT4 and nanog directly regulate dnmt1 to maintain self-renewal and undifferentiated state in mesenchymal stem cells. *Mol Cell* 2012; **47**:169-182.
40 Looijenga LH, Stoop H, de Leeuw HP, *et al.* POU5F1 (OCT3/4) identifies cells with pluripotent potential in human germ cell tumors. *Cancer Res* 2003; **63**:2244-2250.
41 Cantz T, Key G, Bleidissel M, *et al.* Absence of OCT4 expression in somatic tumor cell lines. *Stem Cells* 2008; **26**:692-697.
42 Halfon S, Abramov N, Grinblat B, Ginis I. Markers distinguishing mesenchymal stem cells from fibroblasts are down-regulated with passaging. *Stem Cells Dev* 2011; **20**:53-66.
43 Bae S, Ahn J, Park C, *et al.* Gene and microRNA expression signatures of human mesenchymal stromal cells in comparison to fibroblasts. *Cell Tissue Res* 2009; **335**:565-573.
44 Meng X, Baylink DJ, Sheng M, *et al.* Erythroid promoter confines FGF2 expression to the marrow after hematopoietic stem cell gene therapy and leads to enhanced endosteal bone formation. *PLoS One* 2012; **7**:e37569.
45 Zhang XB, Beard BC, Beebe K, Storer B, Humphries RK, Kiem HP. Differential effects of HOXB4 on nonhuman primate short- and long-term repopulating cells. *PLoS Med* 2006; **3**:e173.

(**Supplementary information** is linked to the online version of the paper on the *Cell Research* website.)